Expansion of a Two-Electron-Population Plasma into Vacuum

G. Hairapetian and R. L. Stenzel
Department of Physics, University of California, Los Angeles, Los Angeles, California 90024-1547
(Received 11 July 1988)

The expansion of a two-electron-population plasma into vacuum is investigated in a controlled laboratory experiment. As the plasma expands, the colder electron population lags behind the energetic tail population, and a potential double layer, called a rarefaction shock, develops where the two separate. Upstream of this double layer, both electron populations exist; but downstream, only the tail electrons do. During the expansion, ions are accelerated to energies well above the tail electron energy.

PACS numbers: 52.30.−q, 52.35.Tc, 52.50.Jm

Plasma expansion plays an important role in laser-fusion[1] and space[2] plasmas (wakes, polar wind, and interhemispheric plasma flows). An interesting characteristic of the expansion is the development of self-consistent electric fields which accelerate ions to high energies. Since detailed *in situ* measurements are not easily feasible in space or laser-fusion plasmas, several laboratory experiments[3] have been carried out to carefully study this phenomenon. Previously, these experiments were limited to Maxwellian, low-density (10^6 cm^{-3} $< n_e < 10^9$ cm^{-3}), single-electron-temperature plasmas. A more interesting case, which occurs in laser-fusion experiments, is the expansion of a plasma with a non-Maxwellian electron distribution[1] (a Maxwellian plus an energetic tail). In our experiment, the expanding discharge plasma has two electron distributions: a Maxwellian ($kT_e \simeq 3$–5 eV) and a shell of energetic electrons ($E \simeq 80$ eV, $n_{\text{tail}}/n_0 \simeq 0.05$). The expansion is along an axial magnetic field, and atomic collisions with background neutrals are negligible. A similar problem with two Maxwellian electron distributions was treated theoretically by Bezzerides, Forslund, and Lindman,[4] who predicted the separation of the hotter electron population from the colder one. The separation is due to higher velocity (energy) of the hot electrons which expand into vacuum first, and set up a space-charge electric field which reflects the cold electrons. The separated electron populations are connected by a double layer referred to as a rarefaction shock. The existence of the rarefaction shock in a two-electron-temperature Maxwellian plasma has since been verified by a number of independent theoretical studies.[5] To our knowledge, no direct experimental observation of the shock has been reported. The purpose of this Letter is first to present experimental evidence of a shocklike structure (double layer) in an expanding two-electron-population plasma, and second to demonstrate that during expansion, ions are accelerated to energies above that of the *tail* electrons ($E \simeq 80$ eV).

The experiment is performed in a large, high-vacuum chamber (80 cm diam, 170 cm length, $P_0 \simeq 2\times10^{-7}$ Torr) shown in Fig. 1. A pulsed ($t_{\text{on}} = 1$ ms, $t_{\text{off}} = 3$ s) supersonic nozzle[6] generates a collimated neutral (Ar) beam that is injected into the chamber radially where it is ionized by energetic discharge electrons ($V_{\text{dis}} \simeq 80$ V, $I_{\text{dis}} \simeq 8$ A) emitted from a filamentary cathode and collected by a grid anode (separation = 0.7 cm). In the vicinity of the cathode, the neutral beam has a density of 1.6×10^{13} cm^{-3} ($P \simeq 5\times10^{-4}$ Torr) and a half width of $\Delta z \simeq 2$ cm as measured with a movable nude ionization gauge[7] (spatial resolution $\simeq 1$ cm). With continuous pumping, the background neutral pressure is controlled by the duty cycle of the pulse gas injection and is typically kept at $\simeq 2\times10^{-6}$ Torr. The pulsed discharge plasma ($n_e \simeq 10^{11}$ cm^{-3}, $kT_e \simeq 3$–5 eV, $kT_i \simeq 0.8$ eV) expands supersonically ($v_{\text{flow}} > 10^6$ cm/s $> c_s \simeq 4\times10^5$ cm/s along an axial magnetic field ($B_z = 35$–45 G) and reaches the end of the chamber ($t_{\text{transit}} \approx 100$ μs) before the slower, radially moving neutrals ($v_{\text{flow}} = 6\times10^4$ cm/s) have a chance to diffuse axially ($t \gg 1$ ms).

The electrons ($r_l = 0.5$ cm) are confined by the external magnetic field to approximately produce a one-dimensional expansion. The very low background pressure makes atomic collisions, both elastic and inelastic, negligible (ion-neutral mean free path, elastic and charge exchange, $l \simeq 30$ m; electron-neutral, $l \simeq 60$ m).[8] This condition is critical in expansion experiments. Ionizing and charge-exchange collisions are restricted to the vicinity of the source, which does not exist in most of the previous laboratory experiments. Once the plasma is created in the source, the energetic tail electrons stream into vacuum along the field lines. Because of their lower velocity, the thermal electrons and ions lag behind the tail electrons. The space-charge separation generates a localized, propagating, self-consistent electric field which slows the electrons and accelerates ions. The effect of the chamber wall on the expansion process is minimized by connection of the cathode to the grounded wall, while the anode and source-plasma potentials are positive at $V \simeq V_{\text{dis}}$. At the backside of the source, a negatively biased electrode is mounted which reflects (absorbs) all incident electrons (ions).

The plasma potential, Φ_p, is measured with an emissive probe (0.1 mm diam, 2 mm long) heated by a pulsed

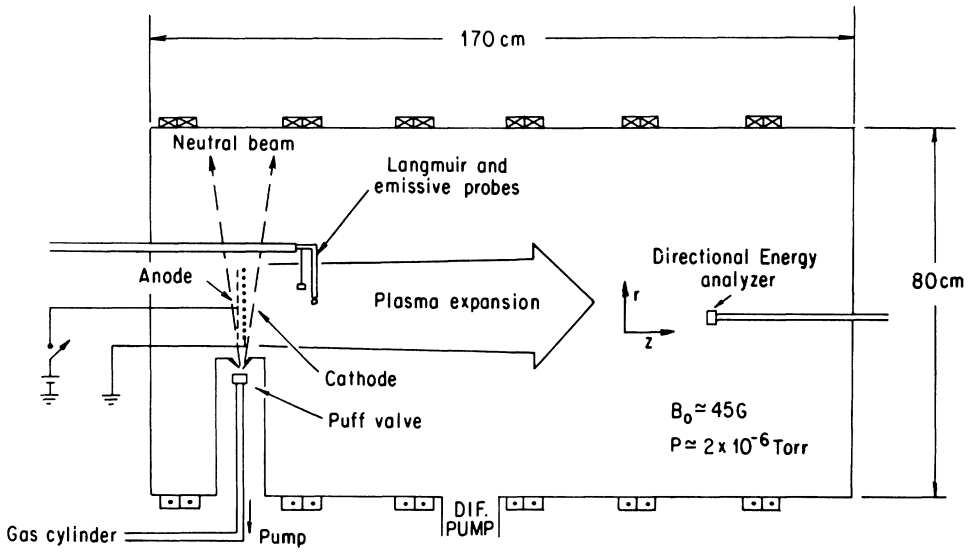

FIG. 1. Schematic side view of the experimental device (not to scale).

dc power supply. The floating potential of the emissive probe is measured with a high-impedance probe ($R=10$ MΩ, $C=10$ pF), while the power supply is disconnected. The emissive probe characteristic is also traced out so as to confirm that the floating potential closely matches the plasma potential ($\Delta\Phi \leq 1.0$ V). The time response of the emissive probe is determined by application of a +100-V pulse (100-ns rise time, 3 μs wide) to a large electrode immersed in the plasma ($\Phi_p = 83$ V) and recording of the time response of the probe. It has been shown[9] that the plasma potential rises with negligible delay throughout the plasma when a large electrode is biased more positively than the plasma potential. The emissive probe is observed to follow the rise and fall of the plasma potential ($\Delta\Phi \simeq 15$ V) with a response time of $t \leq 0.5$ μs in the density regime of 10^9 cm$^{-3} \leq n_e \leq 10^{11}$ cm^{-3}. The potential measurements are performed in one dimension on the central axis of the device over a distance of 100 cm in increments of 2 cm. At each spatial position, the floating potential of the emissive probe as a function time is averaged over ten shots, recorded, and stored for processing in a computer. Subsequently, the plasma potential profiles as a function of time are reconstructed, and differentiated once to yield the electric field profiles ($E_z = -\Delta V/\Delta z$).

Figure 2 shows the time evolution of the plasma potential profile. As a function of time, the potential drop ($\Delta V \simeq 80$ V), set up by the tail electrons ($E \simeq 80$ eV), remains constant while its profile broadens ($\Delta V/\Delta z$ decreases). Since the thermal electrons ($kT_e \simeq 3$–5 eV) are reflected by the potential drop, the expansion front contains mostly the tail electrons. At early times ($t < 40$ μs), the profiles are steep indicating the existence of very large and localized electric fields (80 V/10 cm). As the expansion proceeds, the electric field shown in Fig. 3 propagates, its profile broadens, and its amplitude decreases. At later times ($t \geq 60$ μs), a steplike structure in the potential profile (a double layer, $\Delta V \simeq 30$ V, $\Delta z \simeq 6$ cm) begins to emerge. This propagating double layer, with a zero net current, connects the relatively flat high-potential (80 V), high-density region to a region of low density with a gently decreasing potential profile.

The high-potential region, region I, contains both the tail and the thermal electron population. However, the relative density of the thermal to tail electrons (as measured with a small Langmuir probe) decreases with distance z from the source. Region II, on the other hand, is 25 to 30 V more negative, and contains a very small fraction [$n_e/n_0 = \exp(-30/4) \simeq 5 \times 10^{-4}$] of the thermal electrons which are created near the source at a space

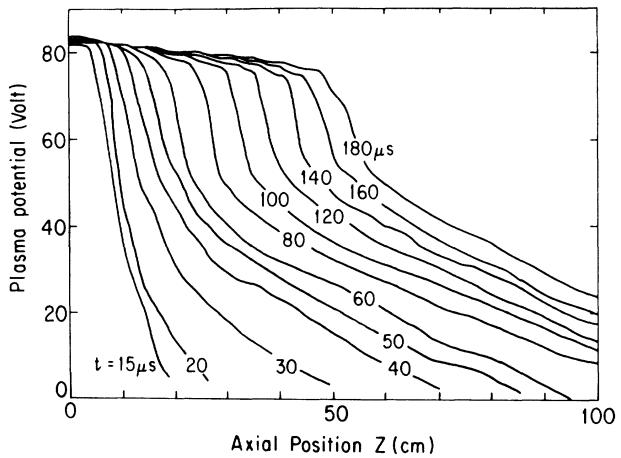

FIG. 2. Measured temporal evolution of the plasma potential profile. $z=0$ corresponds to the position of the source; and $t=0$, to the turn-on of the discharge pulse.

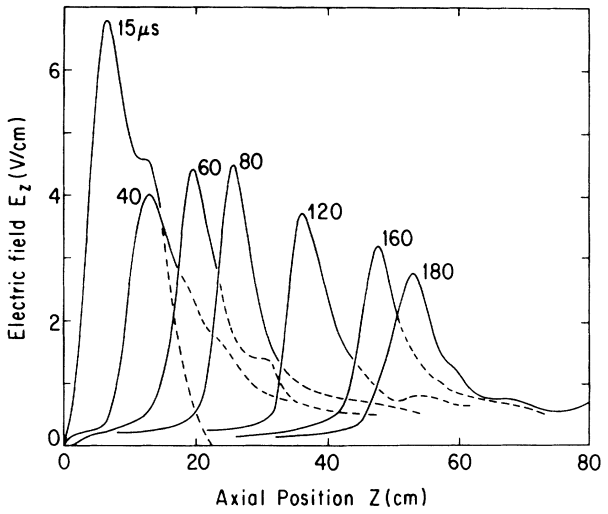

FIG. 3. Electric field profiles as a function of time obtained from first derivatives (dV/dz) of the plasma potential profile (see Fig. 2).

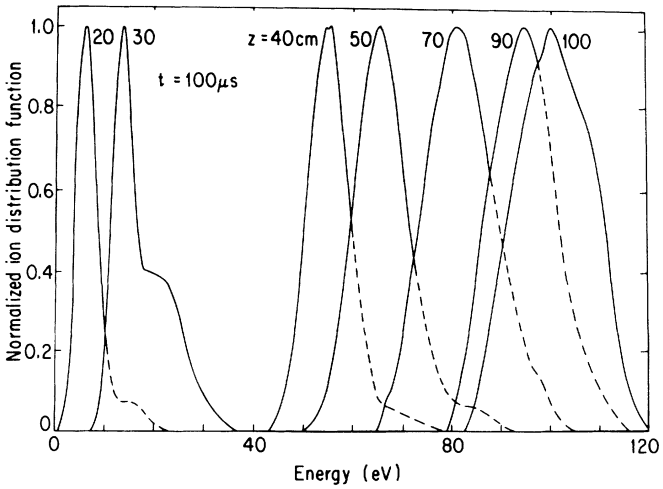

FIG. 4. Normalized ion distribution functions (f/f_{max}) obtained from the first derivatives (dI/dV) of the analyzer characteristics at $t=100$ μs, for several axial positions. The kinetic energy of ions increases with distance z from the source.

potential of 80 V. Thus, the double layer marks the transition between two regions with different electron distribution functions.

One of the most interesting aspects of plasma expansion is the acceleration of ions. The space-charge-generated electric field (as shown above) accelerates ions away from the source. The parallel ion distribution function is mapped out over a distance of 100 cm with a directional retarding-grid energy analyzer[10] (energy resolution=0.5 eV). The directional energy analyzer with a small angular resolution ($\Delta\theta\simeq 6°$) allows us to measure the true velocity-space distribution of ion beams. The knowledge of $f(v)$ is essential in the determination of the energy (velocity) of ions since time-of-flight measurements are inaccurate because of a lack of a well-defined plasma front. The directional analyzer is calibrated to also measure the ion density. At each axial position, the discriminator bias is changed in increments of 0.5 V, and the ion flux versus time is averaged over ten shots, recorded, and stored for each discriminator bias setting. The current-voltage characteristics are reconstructed at each spatial position as a function of time, curve fitted, and then differentiated once to obtain ion distribution functions. Figure 4 shows the normalized ion distribution functions versus energy at $t=100$ μs for several axial positions. Near the source ($z<5$ cm), only the thermal ($kT_i<1$ eV) ions are observed. As the distance from the source increases, the kinetic energy of ions increases, and energetic ion tails begin to develop. A sudden increase in the ion kinetic energy is observed in the vicinity of the double layer ($30<z<40$ cm). As ions traverse across the double layer, they are strongly accelerated by the localized electric field. Downstream of the double layer ($z>40$ cm), the ions have a beamlike distribution function and their kinetic energy increases at an ever decreasing rate. Figure 5 shows the energy and density of ions versus distance from the plasma source (z) at $t=100$ μs. As a function of z, the ion density n_i decreases while the energy increases. At $z=100$ cm, ions reach a streaming energy of 100 eV well in excess of the electron energy (80 eV). The sudden increase in the energy of ions and the corresponding decrease in ion density across the double layer and the subsequent plateau region is clearly evident. The maximum measured ion energy is $E=115$ eV. There exists a continuous spectrum of ion energies with the high-density ($n_i\simeq 10^{11}$ cm^{-3}) thermal ions at the source and the sparse ($n_i\leq 10^9$ cm^{-3}) highly energetic ions at the expansion front.

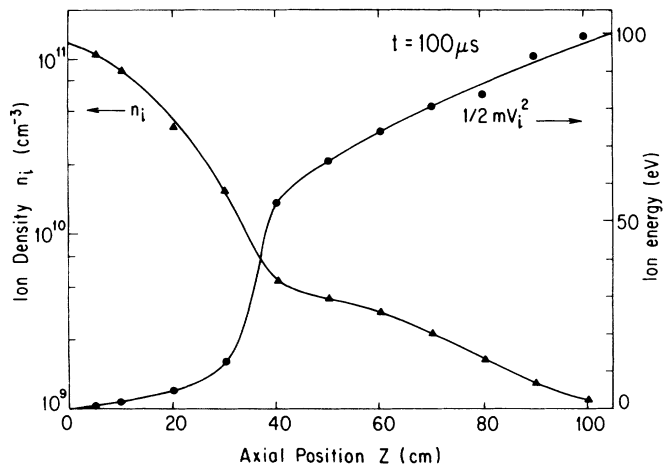

FIG. 5. Ion density and energy profile at $t=100$ μs, showing the sudden increase in the ion energy and a corresponding decrease in the ion density in the vicinity of the double layer.

The intriguing feature of ion acceleration is that ions gain more energy ($E > 110$ eV) than indicated by the electrostatic potential drop (80 V). A careful examination of the temporal evolution of the electric field profiles reveals the explanation. The profiles show that the electric field propagates, and broadens (occupies a larger region) as its amplitude decreases. Thus, the ions are continuously accelerated for a longer length of time as they expand. It must be pointed out again that only a small fraction of ions ($< 1\%$) attain these high energies ($E > 110$ eV).

In summary, we have investigated the expansion of a two-electron-population plasma into vacuum along an axial magnetic field. During expansion, the slower thermal electrons lag behind the faster tail electrons, and the two populations separate. A strong double layer develops across the region where the separation occurs similar to the theoretically predicted rarefaction shock. Ions experience a very strong increase in their energy and a corresponding decrease in their density across this double layer. The moving space-charge electric field accelerates ions to energies above the energy of tail electrons. A quantitative comparison with the existing theories which are limited to Maxwellian plasmas[4,5] is not attempted since in the experiment the energetic electrons have a non-Maxwellian distribution.

The authors acknowledge useful discussions with Dr. J. M. Urrutia, and Dr. D. Diebold and technical assistance from Mr. L. Y. Chan and Mrs. S. Proctor. This work was supported by National Science Foundation Grants No. ATM87-02793 and No. PHY87-13829.

[1]J. S. Pearlman and R. L. Morse, Phys. Rev. Lett. **40**, 1652 (1978); R. Decoste and B. H. Ripin, Phys. Rev. Lett. **40**, 34 (1978).

[2]N. Singh and R. W. Schunk, J. Geophys. Res. **87**, 9154 (1982); U. Samir, K. H. Wright, Jr., and N. H. Stone, Rev. Geophys. Space Phys. **21**, 1631 (1983).

[3]V. G. Eselevich and V. G. Fainshtein, Dokl. Akad. Nauk SSSR **244**, 1111 (1979) [Sov. Phys. Dokl. **24**, 114 (1979)]; C. Chan, N. Hershkowitz, Z. Ferreira, T. Intrator, B. Nelson, and K. Lonngren, Phys. Fluids **27**, 226 (1984).

[4]B. Bezzerides, D. W. Forslund, and E. L. Lindman, Phys. Fluids **21**, 2180 (1978).

[5]J. Denavit, Phys. Fluids **22**, 1384 (1979); A. V. Gurevich and A. P. Meshcherkin, Zh. Eksp. Teor. Fiz. **80**, 1810 (1981) [Sov. Phys. JETP **53**, 937 (1981)]; M. A. True, J. R. Albritton, and E. A. Williams, Phys. Fluids **24**, 1885 (1981).

[6]J. B. Cross and J. J. Valentini, Rev. Sci. Instrum. **53**, 38 (1982).

[7]J. Marshall, in *Proceedings of the Fourth Lockheed Symposium on Magnetohydrodynamics, Plasma Acceleration,* edited by S. W. Kash (Stanford Univ. Press, Stanford, California, 1970), p. 60.

[8]S. C. Brown, *Basic Data of Plasma Physics* (MIT Press, Cambridge, MA, 1966).

[9]J. M. Urrutia and R. L. Stenzel, Phys. Rev. Lett. **57**, 715 (1986).

[10]R. L. Stenzel, R. Williams, R. Aguero, K. Kitazaki, A. Ling, T. McDonald, and J. Spitzer, Rev. Sci. Instrum. **53**, 1027 (1982).